Journal of the Physical Society of Japan
Vol. 51, No. 12, December, 1982, pp. 3900–3907

Self-Consistent Results for a GaAs/$Al_xGa_{1-x}As$ Heterojunction. II. Low Temperature Mobility

Tsuneya ANDO

Institute of Applied Physics, University of Tsukuba, Sakura, Ibaraki 305

(Received July 7, 1982)

The low temperature mobility is calculated in a two-dimensional system at a GaAs/$Al_xGa_{1-x}As$ heterojunction. Scattering mechanisms are assumed to be the Coulomb scattering from ionized donors in the $Al_xGa_{1-x}As$ layer, interface roughness, and scattering caused by alloy disorder present in the $Al_xGa_{1-x}As$ layer. The calculated mobility for the Coulomb scattering explains recent experimental results. The interface roughness and the alloy scattering can play a role at high electron concentrations ($\sim 10^{12}$ cm^{-2}).

§1. Introduction

It is now well-known that extremely high low-temperature mobility can be achieved by the modulation doping technique in a two-dimensional electron gas at a GaAs/$Al_xGa_{1-x}As$ heterojunction.[1-13] Such superior low-temperature transport properties attracted much attention in exploiting its benifits for the implementation of high speed field-effect devices.[14] Extensive experimental studies have been performed to approach maximum mobility. It is also a theoretically interesting problem what can be dominant scattering mechanisms. The purpose of the present paper is to present results of calculation of the low-temperature mobility in this system.

There have been some theoretical investigations on transport properties in GaAs/$Al_xGa_{1-x}As$ systems.[15-21] Scatterings by optical phonons have been discussed by Ferry[15] and Hess.[16] The phonon scattering has also been studied by Basu and Nag[17] and by Price.[19,21] Scatterings by charged centers and screening effects have been discussed by Hess,[16] Price,[20,21] and many others. In case of single quantum wells, Mori and the present author[18] calculated the low-temperature mobility limited by charged centers and interface roughness and studied effects of intersubband scatterings when more than a single subband is occupied by electrons. In this paper the similar method is applied to the present single-heterojunction case. We consider three different scattering mechanisms, i.e., the Coulomb scattering from ionized donors in the $Al_xGa_{1-x}As$ layer, roughness of the interface, and scattering caused by alloy disorder present in the $Al_xGa_{1-x}As$ layer.

In §2 variational wave functions are introduced and the subband structure is discussed and compared with the more exact numerical result. The self-consistency of donor concentrations in the $Al_xGa_{1-x}As$ layer and the electron concentration is also discussed. Mobilities are calculated and results are presented and compared with experiments in §3. It is shown that the calculation which assumes the dominant Coulomb scattering explains recently observed dependence of the mobility on the electron concentration very well. The agreement is satisfactory also for its absolute magnitude. The alloy-disorder scattering is shown to be important at high concentrations especially for systems with a small Al content x. The interface-roughness scattering can also play a role at high electron concentrations. A brief summary and a conclusion are given in §4.

§2. Energy Levels and Wave Functions

In the previous paper,[22] which will be referred to as I in what follows, wave functions and energy levels of subbands have been calculated numerically. For practical purposes, however, it is more convenient to use a variational wave function which enables us to calculate various quantities analytically rather than numerically. The simplest trial function will be

$$\zeta(z)=\begin{cases}(b_0^3/2)^{1/2}z\exp(-b_0z/2) & (z>0),\\ 0 & (z<0),\end{cases} \tag{2.1}$$

with b_0 being a variational parameter. We have chosen the interface of GaAs occupying the right half-space ($z>0$) and $Al_xGa_{1-x}As$ occupying the left half-space ($z<0$) at the xy plane. This function was first proposed by Fang and Howard[23] and has widely been used for Si inversion layers,[24] where the boundary condition that the envelope should vanish at the interface is known to work quite well. In the present system, however, the wave function has a nonvanishing amplitude in the $Al_xGa_{1-x}As$ layer, which can play an important role in certain phenomena. A more elaborate trial function will be

$$\zeta(z)=\begin{cases}Bb^{1/2}(bz+\beta)\exp(-bz/2) & (z>0),\\ B'b'^{1/2}\exp(b'z/2) & (z<0),\end{cases} \tag{2.2}$$

where b, b', β, B, and B' are variational parameters. Among these parameters, β, B, and B' can be expressed in terms of b and b' through boundary conditions at $z=0$ (see eq. (2.1) of I) and the normalization. It is a straightforward task to calculate the total energy $E(b, b')$ in the Hartree approximation. In this paper we confine ourselves to the Hartree approximation which is expected to be sufficient for studying transport properties. The parameters b and b' are determined so as to minimize $E(b, b')$ [but not the subband energy $E_0(b, b')$] numerically.

Figure 1 compares energy levels, wave functions, and potentials calculated by using the functions (2.2) and (2.1) for $x=0.3$, $N_s=5\times10^{11}\,\mathrm{cm}^{-2}$ and $N_{\mathrm{depl}}=5\times10^{10}\,\mathrm{cm}^{-2}$, where N_s is the electron concentration in a unit area and N_{depl} is the concentration of fixed space charges in the GaAs layer. The parameters used in the calculation have been chosen to be same as in I.[22] It is clear that a main effect of the finite barrier height V_0 ($=300$ meV) in the $Al_xGa_{1-x}As$ layer is a simple shift of the average electron position $\langle z\rangle$. The corresponding wave function calculated numerically is also shown in the figure. The subband energy calculated using eq. (2.2) turns out to agree with the numerical result quite well. The agreement is satisfactory also for the relative amplitude of the wave function in the $Al_xGa_{1-x}As$ layer.

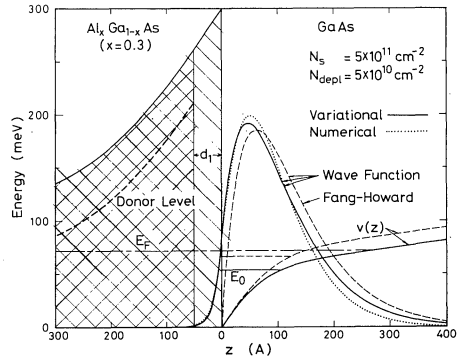

Fig. 1. An example of the wave function, the self-consistent potential, and the bottom of the lowest subband calculated by using variational wave functions. The wave function given by eq. (2.2) gives the solid lines and that given by eq. (2.1) gives the dashed lines. The dotted line represents the wave function calculated numerically. The spacer thickness d_1 is 50 A and the binding energy E_B of donor levels in $Al_xGa_{1-x}As$ is 50 meV.

The function (2.2) gives several % larger values for the average electron position $\langle z\rangle$, as can be seen in Fig. 1. The both variational wave functions (2.1) and (2.2) tend to have larger amplitude than the exact numerical one for large z. In any case, the present variational functions, especially given by eq. (2.2), are sufficient for the calculation of the mobility as long as only the lowest subband is occupied by electrons. Effects of intersubband scatterings which play important roles when more than a single subband is occupied is not explicitly taken into account in this paper. We will return to this problem in §4.

When the two-dimensional system is in equilibrium with the donor levels in the $Al_xGa_{1-x}As$ layer, we have the condition:

$$E_0+E_F=V_0-E_B-\frac{4\pi e^2}{\kappa}\frac{1}{2}(N_D'-N_A')d_2^2 -\frac{4\pi e^2}{\kappa}(N_s+N_{\mathrm{depl}})d_1+\frac{4\pi e^2}{\kappa}N_s\frac{B'^2}{b'}, \tag{2.3}$$

where κ is the static dielectric constant, d_1 is the thickness of the undoped $Al_xGa_{1-x}As$ layer (sometimes called the spacer), d_2 is the thickness of the $Al_xGa_{1-x}As$ layer containing ionized donors, N_D' and N_A' are donor and acceptor concentrations, and $-E_B$ is the energy of a donor measured from the bottom of the $Al_xGa_{1-x}As$ conduction band. The last term

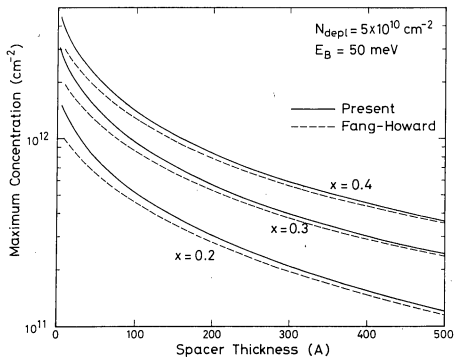

Fig. 2. Maximum available electron concentrations as a function of the spacer thickness d_1 for different values of the Al content x. The solid lines and dashed lines are obtained by using wave functions given by eqs. (2.2) and (2.1), respectively.

of the right hand side of eq. (2.3) appears because the electron density is nonzero in the $Al_xGa_{1-x}As$ layer and should be dropped for the wave function (2.1). The subband energy E_0 measured from the bottom of the conduction band of GaAs at $z=0$ is a function of only N_s, N_{depl}, and V_0 in a good approximation. The Fermi energy E_F is measured from the bottom of the lowest subband E_0. The charge neutrality requires

$$(N'_D-N'_A)d_2=N_s+N_{depl}, \tag{2.4}$$

which determines together with eq. (2.3) the equilibrium value of $N'_D-N'_A$ and d_2 for a fixed value of N_s and N_{depl}.

For each d_1 there is an upper limit in the concentration of electron which can be stored in the two-dimensional system in equilibrium with donor levels in the $Al_xGa_{1-x}As$ layer. This upper limit can be obtained by taking the limit $d_2\to0$ and $N'_D-N'_A\to\infty$ with their product being kept fixed in eq. (2.3). Figure 2 shows an example of such upper limits as a function of the spacer thickness d_1 for different values of the Al content x. The binding energy E_B of a Si donor in $Al_xGa_{1-x}As$, which has not exactly been known experimentally, is chosen to be 50 meV in this figure. Extremely heavy doping is necessary to achieve electron concentrations near such upper limits (see also Fig. 4).

§3. Low Temperature Mobility

3.1 *Coulomb scattering*

The relaxation time for scattering from charged centers is given by[24]

$$\frac{\hbar}{\tau_C(k)}=2\pi\int dz\, N_i(z)\sum_q\left[\frac{2\pi e^2}{q\varepsilon(q)}\right]^2|F_i(q,z)|^2 \times(1-\cos\theta)\delta(\varepsilon_k-\varepsilon_{k-q}), \tag{3.1}$$

with $q=2k\sin(\theta/2)$ and $\varepsilon_k=\hbar^2k^2/2m$ where k is the wave vector, θ is the scattering angle, and m is the effective mass of GaAs. The static dielectric function of the two-dimensional electron gas is given by

$$\varepsilon(q)=1+\frac{2\pi e^2}{\kappa q}\frac{2m}{2\pi\hbar^2}F(q), \tag{3.2}$$

for $q<2k_F$ where k_F is the Fermi wave vector. The form factors are defined as

$$F_i(q,z)=\int dz'\,|\zeta(z')|^2\exp(-q|z-z'|), \tag{3.3}$$

$$F(q)=\int dz\int dz'\,|\zeta(z)|^2|\zeta(z')|^2\exp(-q|z-z'|), \tag{3.4}$$

which can easily be calculated for the wave functions (2.1) and (2.2). The impurity distribution $N_i(z)$ is assumed to be

$$N_i(z)=\begin{cases}0 & (-d_1<z),\\ N'_D+N'_A & (-d_1-d_2<z<-d_1),\\ 2N'_A & (z<-d_1-d_2).\end{cases} \tag{3.5}$$

Since the contribution of charged centers which are far apart from the interface ($|z_i|\gg k_F^{-1}$, where $|z_i|$ is the distance from the interface) is exponentially small, the relaxation time is determined by $N'_D+N'_A$ and does not depend on d_2 except in the case that d_2 is extremely small, i.e., except when the electron concentration is close to the upper limit discussed in the previous section. The compensation of Si donors in $Al_xGa_{1-x}As$ has not been known exactly.

An example of calculated mobilities at zero temperature is given in Fig. 3 as a function of N_s for different values of the thickness d_1 of the undoped layer. We have assumed that $N_{depl}=5\times10^{10}$ cm^{-2}, $E_B=50$ meV, and $K=0.25$, where $K=N'_A/N'_D$ is the compensation and we have determined N'_D and N'_A using eqs. (2.3) and (2.4). The corresponding results for $N'_D-N'_A$ are given in Fig. 4.

In the case $N_s\ll N_{depl}$, a small increase in $N'_D-N'_A$ is sufficient to increase the electron concentration and the mobility increases with N_s because the increase of the electron kinetic energy reduces the strength of scattering from

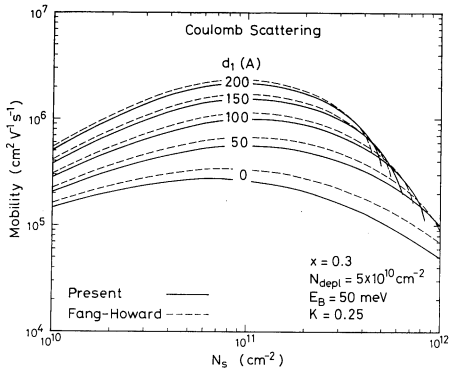

Fig. 3. An example of calculated mobility limited by charged centers in the $Al_xGa_{1-x}As$ layer. The sold lines and dashed lines are obtained by using wave functions given by eqs. (2.2) and (2.1), respectively. At each electron concentration N_s, the effective doping N_D'-N_A' is determined by the charge neutrality condition and the equilibrium condition between the electron system and donor levels in the $Al_xGa_{1-x}As$ layer. The total concentration of charges, $N_D'+N_A'$, is determined by assuming $K=N_A'/N_D'=0.25$.

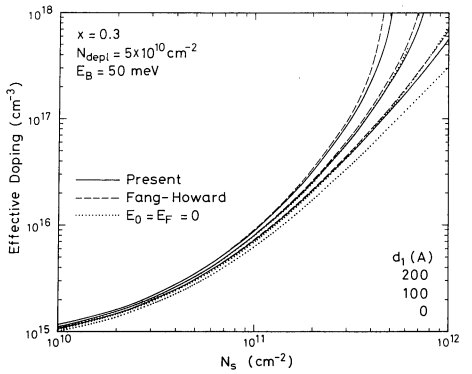

Fig. 4. An example of calculated effective doping $N_D'-N_A'$ as a function of the electron concentration for the spacer thickness $d_1=0$, 100, and 200 A. The solid lines and dashed lines are obtained by using wave functions given by eqs. (2.2) and (2.1), respectively. The dotted lines are obtained by putting $E_F=E_0=0$ and neglecting the band bending due to the two-dimensional electron gas.

each impurity as well as the number of impurities which are effective in scattering. As shown in Fig. 4, however, the doping level should increase much faster and the mobility starts to decrease with N_s in the case $N_s>N_{depl}$. The behavior is quite different from that in superlattices or quantum wells in which the mobility increases with the concentration except at low electron concentrations.[16] In case of quantum wells N_s increases in proportional to $N_D'-N_A'$, whereas in the present case N_s increases more slowly as is shown in Fig. 4 when $N_s \gg N_{depl}$.

The another important feature is that the mobility becomes higher for larger spacer thickness d_1 except near the upper limits of the electron concentration although the doping level $N_D'-N_A'$ is larger. This demonstrates the effectiveness of the modulation doping in achieving a higher mobility.

Figure 5 shows an example of calculated mobilities for a fixed value of the doping level, i.e. $N_D'-N_A'=2\times10^{17}\ cm^{-3}$. The other parameters are the same as in Figs. 3 and 4. The mobility μ depends on N_s like $\mu \propto N_s^{\gamma}$ where $\gamma\sim1$ for $d_1=0$ and $\gamma\sim1.5$ for $d_1=200$ A. The figure contains experimental results of Tsui *et al.*,[12] who fabricated insulated-gate field effect transistors with different d_1's and showed that γ increased from ~0.5 at $d_1=0$ to ~1.4 at $d_1=165$ A. The calculated value of γ for large spacer thickness d_1 agrees quite well with the experiments. For the vanishing thickness, however, the experiments give much smaller γ. A possible diffusion of donor impurities into the GaAs layer might be responsible for this disagreement. Other scattering mechanisms can also be another candidate. Hiyamizu *et al.*[25] increased the electron con-

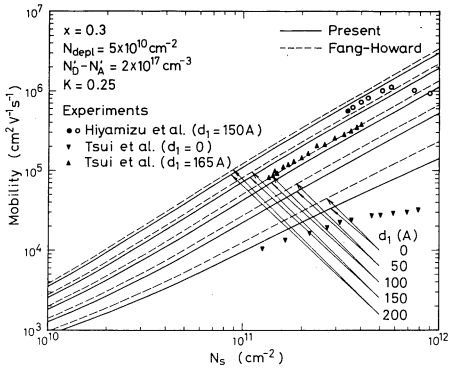

Fig. 5. An example of calculated mobilities limited by charged centers in the $Al_xGa_{1-x}As$ layer for a fixed concentration of charged centers. The solid lines and dashed lines are obtained by using wave functions given by eqs. (2.2) and (2.1), respectively. Experimental results of Hiyamizu *et al.*[25] and of Tsui *et al.*[12] are also shown. The effective doping $N_D'-N_A'=2\times10^{17}\ cm^{-2}$ has been chosen to account for the electron concentration under the equilibrium condition (the black dot) observed by Hiyamizu *et al.*[25] The circles have been obtained under light exposure.

centration by exposing the system to band-gap radiations. The results are also plotted in Fig. 5. The experiments can be explained if we assume that the radiation does not influence the concentration of charged impurities in the vicinity of the interface and that its main effect is to simply increase the electron concentration. The doping level $N'_D - N'_A = 2\times 10^{17}$ cm^{-2} roughly corresponds to the equilibrium electron concentration (the black dot in Fig. 5) observed by Hiyamizu *et al.*[25] Therefore, the agreement is satisfactory even concerning the absolute value.

Hiyamizu and associates[5] showed that $N_s \propto N_{Si}^{1/2}$ between $N_s = 2\times 10^{11}$ and 10^{12} cm^{-2} for $d_1 = 60$ A in qualitative agreement with Fig. 4, where N_{Si} is the concentration of doped Si in $Al_xGa_{1-x}As$. Quantitatively, however, only 10% of doped Si atoms contribute to the effective doping $N'_D - N'_A$ which determines the electron concentration in our system. On the other hand, the magnitude of the observed mobilities is explained by assuming relatively small compensation ($K \sim 0.3$) as is shown in Fig. 5. Therefore, we have to conclude that most of doped Si forms neutral (deep) levels and only 10% of Si atoms become shallow donors in the $Al_xGa_{1-x}As$ layer.

3.2 *Interface-roughness scattering*

The relaxation time for interface-roughness scattering is given by the same expression as that for Si inversion layers:[24]

$$\frac{\hbar}{\tau_{IR}(k)} = 2\pi \sum_q \pi \left[\frac{\Delta\Lambda F_{eff}}{\varepsilon(q)}\right]^2 \exp\left(-\frac{1}{4}q^2\Lambda^2\right) \times (1-\cos\theta)\delta(\varepsilon_k - \varepsilon_{k-q}). \quad (3.6)$$

Here, we have defined the effective field F_{eff} by

$$F_{eff} \equiv \int dz\, |\zeta(z)|^2 \frac{\partial v(z)}{\partial z} = \frac{4\pi e^2}{\kappa}\left(\frac{1}{2}N_s + N_{depl}\right), \quad (3.7)$$

where $v(z)$ is the electrostatic potential [$v_H(z)$ in I] and the overlapping of the wave function with the $Al_xGa_{1-x}As$ layer where donors are ionized is neglected in the last equality. The roughness $\Delta(\boldsymbol{r})$ has been assumed to have the correlation function,

$$\langle \Delta(\boldsymbol{r})\Delta(\boldsymbol{r}')\rangle = \Delta^2 \exp(-|\boldsymbol{r}-\boldsymbol{r}'|^2/\Lambda^2), \quad (3.8)$$

where $\langle\cdots\rangle$ means an average, Δ is the mean-square deviation of the height, and Λ is the lateral spatial decay rate of the roughness. It should be noted that eq. (3.6) is applicable to heterojunctions characterized by much more complicated boundary conditions like InAs/GaSb systems[26] as long as change in the electrostatic potential caused by the roughness can be neglected. Note also that the strength of the interface-roughness scattering is independent of the barrier height and therefore the value of x and solely depends on the values of Δ and Λ. Further the product $\Delta\Lambda$ is the important parameter as long as the wave length of electrons $2\pi/k_F$ is much larger than Λ.

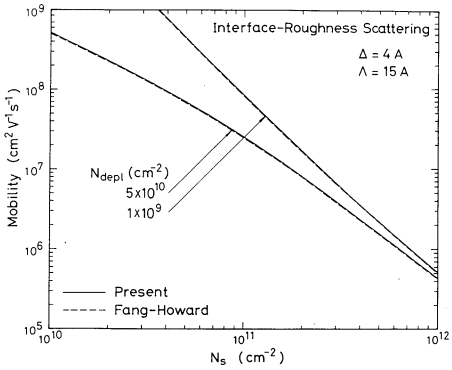

Fig. 6. An example of calculated mobilities limited by interface-roughness scattering for the mean deviation $\Delta = 4$ A and the lateral decay rate $\Lambda = 15$ A. The solid lines and dashed lines are obtained by using wave functions given by eqs. (2.2) and (2.1), respectively.

An example of calculated results for $x = 0.3$ is shown in Fig. 6, where the mobility is plotted against N_s for $N_{depl} = 5\times 10^{10}$ and 1×10^9 cm^{-2}. The parameters used in the calculation are $\Delta = 4$ A and $\Lambda = 15$ A, which are typical roughness parameters used for explaining the mobility in Si inversion layers at high concentrations like $N_s \sim 10^{13}$ cm^{-2}.[27] The comparison of the results for the two wave functions (2.1) and (2.2) clearly demonstrates the independence of the mobility on the barrier height or the Al content x mentioned above. The figure demonstrates that the roughness can be effective in determining the mobility at electron concentrations as high as $N_s \sim 10^{12}$ cm^{-2}. However, the roughness might be expected to be smaller in the present system than in Si/SiO_2 systems.

3.3 Alloy-disorder scattering

As is shown in Fig. 1 the wave function has a nonvanishing amplitude in the $Al_xGa_{1-x}As$ layer. Therefore, an electron can suffer from scattering due to alloy disorder in the layer. The band structure of III-V compounds is well reproduced by a linear combination of s, p_x, p_y, and p_z orbitals in the nearest neighbor empirical tight-binding approximation.[28] Especially, the conduction band edge is described by an s orbital on the anion site. This means that the potential of Al and Ga can be replaced by a short-range δ-potential with the strength $(1-x)\Delta E_c(a^3/4)$ and $-x\Delta E_c(a^3/4)$, respectively, where ΔE_c is the difference of the conduction band minima of AlAs and GaAs, a is the lattice constant, and the factor (1/4) appears because a cubic unit cell contains four anion sites. The relaxation time for the alloy-disorder scattering is given by

$$\frac{\hbar}{\tau_{AD}(k)} = 2\pi x(1-x)\frac{a^3}{4}\Delta E_c^2 \int_{-\infty}^{0} dz\,|\zeta(z)|^4 \times \sum_q \frac{1-\cos\theta}{\varepsilon(q)^2}\delta(\varepsilon_k - \varepsilon_{k-q}). \tag{3.9}$$

Figure 7 gives the mobility limited by this mechanism for $x=0.1$, 0.2, 0.3, and 0.4 and for $N_{depl}=5\times10^{10}$ cm^{-2} and 1×10^{9} cm^{-2}. We have assumed $\Delta E_c=1$ eV and used the wave function (2.2). The figure shows that the alloy scattering can be a dominant scattering mechanism at high electron concentrations especially for small x. In addition, the two facts are noteworthy: First, the mobility depends on the Al content x and increases with x. Second, its dependence on N_s and N_{depl} is quite similar to that of the mobility limited by the interface roughness. These features can be understood as follows. Since the effect of the discontinuity in the envelope function at the interface is small as is shown in Fig. 1, we use the simple boundary condition that it is smooth across the interface. When the barrier height V_0 is sufficiently large, the wave function for $z<0$ is approximately give by $\zeta(z)\sim\zeta(0)\exp[(2mV_0/\hbar^2)^{1/2}z]$. Therefore, the strength of scattering $1/\tau_{AD}$ is proportional to $|\zeta(0)|^4V_0^{-1/2}$. On the other hand, the condition that the total force acting on an electron must vanish gives $V_0|\zeta(0)|^2+\langle\partial v(z)/\partial z\rangle=0$. Therefore, we get

$$\frac{1}{\tau_{AD}} \propto \frac{x(1-x)}{V_0^{5/2}}F_{eff} \propto \frac{(1-x)}{x^{3/2}}\left(\frac{1}{2}N_s+N_{depl}\right), \tag{3.10}$$

which explains the two characteristic features mentioned above.

The calculated mobility shown in Fig. 7 has become smaller than observed by Hiyamizu *et al.*[25] given in Fig. 5. Note, however, that the present model of the alloy disorder scattering can predict only the order of magnitude of the scattering. Equation (3.9) is based on the simplest nearest-neighbor LCAO approximation for the band structure. From a microscopic stand point, the boundary layer of GaAs and $Al_xGa_{1-x}As$ consists of Ga and Al atoms distributed randomly even in ideal interfaces. Fluctuations in the interface position having a spatial dimension much larger than the lattice constant can certainly be considered separately from the alloy disorder. However, it is not possible to distinguish between the interface roughness and the alloy disorder when the fluctuation is comparable to the lattice constant. The present effective-mass approximation is inappropriate and more microscopic theory is necessary to deal with these problems.

Scatterings due to disorder in amorphous SiO_2 have been discussed by Stern in case of Si inversion layers.[29] Stern argued, however, the scattering strength is proportional to the portion of the electron density in SiO_2, whereas it is proportional to the fourth power of the amplitude in the $Al_xGa_{1-x}As$ layer in the present case.

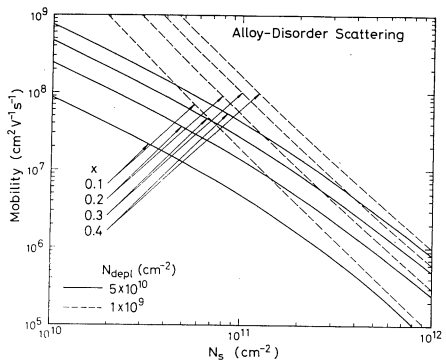

Fig. 7. An example of calculated mobilities limited by alloy-disorder scattering for different values of the Al content x. The both solid and dashed lines are obtained by using the wave function (2.2).

§4. Discussion and Conclusion

So far we have ignored the fact that excited subbands become occupied by electrons at high electron concentrations. As has been shown in I,[22] the Fermi level reaches the bottom of the second subband at $N_s=7.3\times 10^{11}\ \mathrm{cm}^{-2}$ for $N_{\mathrm{depl}}=5\times 10^{10}\ \mathrm{cm}^{-2}$ and at $N_s=3\times 10^{11}\ \mathrm{cm}^{-2}$ for $N_{\mathrm{depl}}=1\times 10^{9}\ \mathrm{cm}^{-2}$. When the Fermi level lies in excited subbands, intersubband scatterings can become important. As has been shown above, the finite barrier height of the $Al_xGa_{1-x}As$ layer does not play an essential role in determining the mobility limited by the Coulomb and interface-roughness scatterings. Therefore, results of a previous work for Si inversion layers[30] are expected to be valid in the present system. It has been shown that electrons in excited subbands have a mobility much higher than that in the lowest subband. However, strong intersubband scatterings reduce the mobility of the lowest subband from that in the single-subband case. The latter effect dominates the former and the net average mobility becomes smaller when excited subbands become populated by electrons.

As shown in Fig. 5 the mobilities observed by both Tsui *et al.*[12] and Hiyamizu *et al.*[25] have the tendency of decreasing with N_s at high electron concentrations. This fact might be explained by effects of intersubband scatterings. As has been shown, however, other scattering mechanisms can also be important at high electron concentrations. In order to distinguish between these two effects, combined experiments of the mobility and Shubnikov-de Haas oscillations are highly desirable.

We have calculated the low temperature mobility in a two-dimensional system at $GaAs/Al_xGa_{1-x}As$ heterojunctions. Two trial wave functions have been used. The simpler one corresponds to the infinitely high barrier in the $Al_xGa_{1-x}As$ layer and the other more accurate one includes effects of nonvanishing amplitude in the layer. It has been demonstrated that the Coulomb scattering from ionized donors in the $Al_xGa_{1-x}As$ layer depends on the thickness d_1 of the spacer and the electron concentration strongly. Especially the mobility has been shown to be expressed as $\mu\propto N_s^{\gamma}$ where $\gamma\sim 1$ for $d_1=0$ and $\gamma\sim 1.5$ for $d_1=200$ A, in qualitative agreement with recent experiments. Interface roughness has been shown to play a role at high electron concentrations. The two wave functions give similar results for the both Coulomb and interface-roughness scatterings. Effects of alloy-disorder have been shown to be more important and can dominate at high electron concentrations especially for small x.

Acknowledgments

The numerical computation has been performed with the aid of FACOM M200 at the University of Tsukuba. This work is partially supported by the Grant-in-Aid for Scientific Research from the Ministry of Education.

References

1) R. Dingle, H. L. Störmer, A. C. Gossard and W. Wlegmann: Appl. Phys. Lett. **33** (1978) 665.
2) H. L. Störmer, R. Dingle, A. C. Gossard, W. Wiegmann and M. D. Sturge: Solid State Commun. **29** (1979) 705; J. Vac. Sci. & Technol. **16** (1979) 1517.
3) S. Hiyamizu, T. Mimura, T. Fujii and K. Nanbu: Appl. Phys. Lett. **37** (1980) 805.
4) S. Hiyamizu, T. Mimura, T. Fujii, K. Nanbu and H. Hashimoto: Jpn. J. Appl. Phys. **20** (1981) L245.
5) S. Hiyamizu, T. Mimura and T. Ishikawa: *Proc. 13th Int. Conf. Solid State Devices, Tokyo, 1981*, Jpn. J. Appl. Phys. **21** (1981) Suppl. 21-1, p. 161.
6) H. Morkoc, L. C. Witkowski, T. J. Drummond, C. M. Stanchak, A. Y. Cho and B. G. Streetman: Electron. Lett. **16** (1980) 753.
7) L. C. Witkowski, T. J. Drummond, C. M. Stanchak and H. Morkoc: Appl. Phys. Lett. **37** (1980) 1033.
8) L. C. Witkowski, T. J. Drummond, S. A. Barnett, H. Morkoc, A. Y. Cho and J. E. Greene: Electron. Lett. **17** (1981) 126.
9) T. J. Drummond, H. Morcoc and A. Y. Cho: J. Appl. Phys. **52** (1981) 1380.
10) T. J. Drummond, H. Morkoc, K. Hess and A. Y. Cho: J. Appl. Phys. **52** (1981) 5231.
11) T. J. Drummond, W. Kopp, H. Morkoc, K. Hess, A. Y. Cho and B. G. Streetman: J. Appl. Phys. **52** (1981) 5231.
12) D. C. Tsui, A. C. Gossard, G. Kaminski and W. Wiegmann: Appl. Phys. Lett. **39** (1981) 712.
13) H. L. Störmer, A. C. Gossard, W. Wiegmann and K. Baldwin: Appl. Phys. Lett. **39** (1981) 912.
14) See, for example, T. Mimura: Surf. Sci. **113** (1982) 454.
15) D. K. Ferry: Surf. Sci. **75** (1978) 86.
16) K. Hess: Appl. Phys. Lett. **35** (1979) 484.
17) P. K. Basu and B. R. Nag: Phys. Rev. **B22** (1980) 4849.
18) S. Mori and T. Ando: J. Phys. Soc. Jpn. **48** (1980)

865; Surf. Sci. **98** (1980) 101.
19) P. J. Price: Ann. Phys. (USA) **133** (1981) 217.
20) P. J. Price: J. Vac. Sci. & Technol. **19** (1981) 599.
21) P. J. Price: Surf. Sci. **113** (1982) 199.
22) T. Ando: J. Phys. Soc. Jpn. **51** (1982) 3893.
23) F. F. Fang and W. E. Howard: Phys. Rev. Lett. **16** (1966) 797.
24) See, for example, T. Ando, A. B. Fowler and F. Stern: Rev. Mod. Phys. **54** (1982) 437.
25) S. Hiyamizu, J. Saito, K. Nanbu, T. Ishikawa. T. Mimura and H. Hashimoto: to be published.
26) See, for example, L. L. Chang and L. Esaki: Surf. Sci. **98** (1980) 70 and references cited therein.
27) See, for example, T. Ando: J. Phys. Soc. Jpn. **43** (1977) 1616 and references cited therein.
28) D. J. Chadi and M. L. Cohen: Phys. Status Solidi (b) **68** (1975) 405.
29) F. Stern: Solid State Commun. **21** (1977) 163.
30) S. Mori and T. Ando: Phys. Rev. B**19** (1979) 6433.